Addressing Transient Errors in Passive Macromodels of Distributed Transmission-Line Networks

Anestis Dounavis, *Student Member, IEEE,* Ramachandra Achar, *Member, IEEE,* and Michel S. Nakhla, *Fellow, IEEE*

***Abstract*—Recently, several time-domain passive macromodeling algorithms were proposed for distributed transmission-line networks. Most of them employ some kind of approximation in the frequency domain to match the response up to a maximum frequency of interest and the behavior after the highest frequency is generally not considered. This can cause significant errors in transient responses (especially in the early-time period). In order to address this difficulty, we will present a new algorithm to reduce high-frequency errors in time-domain macromodels, while preserving passivity. The proposed algorithm is very useful in eliminating spurious ripples in the flat delay portion of transient responses of distributed transmission-line networks without needing to increase the order of approximation.**

***Index Terms*—Circuit simulation, distributed networks, high-speed interconnects, model-reduction, printed circuit boards, transient analysis, transmission lines.**

I. Introduction

THE ever-increasing quest for higher operating speeds, miniature devices, and denser layouts has made the interconnect effects such as delay, crosstalk, ringing and distortion, the dominant factors limiting the overall performance of microelectronic/microwave systems. At higher frequencies, the length of the interconnect becomes a significant fraction of the operating wavelength, so conventional lumped-impedance models become inadequate and distributed transmission-line models become necessary [1]–[12]. However, simulation of distributed transmission lines in the presence of nonlinear elements suffers from the mixed frequency/time difficulty. There are several techniques available in the literature to address this problem. Broadly speaking, they can be classified into two categories. The first includes techniques based on the generalized method of characteristics (MC) [3]–[5]. The second category is based on passive macromodeling of transmission lines [7]–[10].

In general, MC extracts the line delay and a transfer-function characterizing the frequency response of the line. An important advantage of the MC approach is that, since it extracts the line delay explicitly, the corresponding transient responses generally do not exhibit spurious ripples in the early-time region. However, the MC can be CPU expensive in the presence of nonlinear elements and lossy lines. In addition, it does not guarantee the passivity of macromodels. Passivity is an important property to satisfy because macromodels that are stable but not passive can produce unstable networks when connected to other stable, even passive loads. This can lead to faulty transient simulation.

On the other hand, recently published passive macromodeling schemes [7]–[10] guarantee the passivity of macromodels, and lead to macromodels in terms of ordinary differential equations. Most of these algorithms employ some kind of approximation in the frequency-domain to match the impulse response up to a maximum frequency of interest ($f_{\max}$). However, the behavior after $f_{\max}$ is generally not considered, which can lead to significant errors in the impulse transient response, especially in the early-time period (spurious ripples) [11], [12]. This can affect the accuracy of the transient response at all other time points when the macromodel is included during the simulation of a large network. Also, the above problem can be aggravated in the presence of sharp rise times or with smaller capacitive loads. To remove these ripples, the order of the approximation required would be very high, making the macromodel inefficient.

In order to address the above problem of faulty transient response due to high-frequency errors, a new algorithm is presented in this paper. The proposed algorithm provides a mechanism to control the asymptotic behavior of high-frequency impulse response while matching the response up to $f_{\max}$ accurately. This leads to significant reduction in errors of transient responses. Also, it guarantees the passivity of the macromodel. The proposed algorithm achieves the above objectives with macromodel orders comparable to the ones published in the literature. The macromodel is obtained analytically, in terms of predetermined (stored) constants and the given per-unit length (PUL) line parameters. Numerical examples are presented to demonstrate the validity, accuracy and efficiency of the proposed method.

II. Review of Distributed-Transmission-Line Macromodeling

A. Transmission-Line Equations

Distributed interconnects are described by a set of partial differential equations known as Telegrapher's equations

$$\begin{aligned}\frac{\partial}{\partial x}\boldsymbol{v}(x,t) &= -\boldsymbol{R}\boldsymbol{i}(x,t) = -\boldsymbol{L}\frac{\partial}{\partial t}\boldsymbol{i}(x,t)\\ \frac{\partial}{\partial x}\boldsymbol{i}(x,t) &= -\boldsymbol{G}\boldsymbol{v}(x,t) = -\boldsymbol{C}\frac{\partial}{\partial t}\boldsymbol{v}(x,t)\end{aligned} \tag{1}$$

where $\boldsymbol{R}$, $\boldsymbol{L}$, $\boldsymbol{G}$, and $\boldsymbol{C} \in \Re^{\psi\times\psi}$ are the PUL parameters of the transmission line, $\boldsymbol{v}(x,t)$, $\boldsymbol{i}(x,t) \in \Re^{\psi}$ represent the voltage and current vectors as a function of position x and time t, and

Manuscript received April 5, 2002; revised August 22, 2002.

The authors are with the Department of Electronics, Carleton University, Ottawa, ON, Canada K1S 5B6 (e-mail: msn@doe.carleton.ca)

Digital Object Identifier 10.1109/TMTT.2002.805130

$\psi+1$ is the number of lines including the reference line. Equation (1) can be written in the Laplace domain as

$$\begin{bmatrix} \boldsymbol{V}(d,s) \\ -\boldsymbol{I}(d,s) \end{bmatrix} = e^{\boldsymbol{Z}} \begin{bmatrix} \boldsymbol{V}(0,s) \\ \boldsymbol{I}(0,s) \end{bmatrix}$$
$$\boldsymbol{Z} = \begin{bmatrix} \boldsymbol{0} & -(\boldsymbol{R}+s\boldsymbol{L})d \\ -(\boldsymbol{G}+s\boldsymbol{C})d & \boldsymbol{0} \end{bmatrix} \quad (2)$$

where $\boldsymbol{V}(s)$ and $\boldsymbol{I}(s)$ are the terminal voltage and current vectors of the transmission line and d is the length of the line. Equation (2) does not have a direct representation in the time domain, which makes it difficult to interface with nonlinear simulators. In [7]–[10], passive macromodeling schemes have been proposed to address the issue of mixed frequency/time simulation. These methods efficiently capture the frequency response between (0 and $f_{\max}$); however, the algorithms are susceptible to spurious early-time ripples due to the frequency behavior beyond $f_{\max}$. This can affect the accuracy of the transient response at all other time points when the macromodels are included in large networks. In order to address the above problem, a new algorithm is presented which controls the asymptotic behavior of the high-frequency response using the matrix-rational approximation (MRA) algorithm [8] as an example. For this purpose, a brief review of the MRA-based macromodeling is given in Section II-B. However, note that the principles stated in this paper are general in nature and they can also be included in other rational-function-based passive macromodeling algorithms available in the literature, with appropriate modifications.

B. Review of MRA-Based Passive Macromodels

The exponential matrix $e^{\boldsymbol{Z}}$ in (2) can be expressed with a matrix rational approximation as

$$\boldsymbol{P}_M(\boldsymbol{Z})e^{\boldsymbol{Z}} \approx \boldsymbol{Q}_N(\boldsymbol{Z})$$
$$\boldsymbol{P}_M(\boldsymbol{Z}) = \sum_{i=0}^{M} p_i \boldsymbol{Z}^i$$
$$\boldsymbol{Q}_N(\boldsymbol{Z}) = \sum_{i=0}^{N} q_i \boldsymbol{Z}^i \quad (3)$$

where $\boldsymbol{P}_M(\boldsymbol{Z})$ and $\boldsymbol{Q}_N(\boldsymbol{Z})$ are polynomial matrices. The above approximation is formulated analytically in terms of predetermined constants (i.e., q_i and p_i) and PUL parameters. The following theorem was used in [8] to show that for $M=N$, passive macromodels can be obtained.

Theorem 1: Let the rational approximation of e^s be

$$e^s \approx \frac{Q(s)}{Q(-s)} = \frac{\sum_{i=0}^{N} q_i s^i}{\sum_{i=0}^{N} q_i s^i} = \frac{\mathrm{Ev}(Q)+\mathrm{Odd}(Q)}{\mathrm{Ev}(Q)-\mathrm{Odd}(Q)}$$
$$\mathrm{Ev}(Q) = \sum_{i=0}^{N} q_i \left[\frac{1}{2}(1+(-1)^i)s^i\right]$$
$$\mathrm{Odd}(Q) = \sum_{i=0}^{N} q_i \left[\frac{1}{2}(1-(-1)^i)s^i\right] \quad (4)$$

where the polynomial $Q(s)$ is strictly Hurwitz. *If the above conditions are satisfied, then the rational matrix obtained by replacing the scalar s with the matrix $\boldsymbol{Z}$ of* (2) *results in a passive transmission-line macromodel.* Next, knowing the coefficients q_i, we can write the macromodel of the multiconductor transmission-line as

$$\begin{bmatrix} \boldsymbol{Q}_{11} & -\boldsymbol{Q}_{12} \\ -\boldsymbol{Q}_{21} & \boldsymbol{Q}_{22} \end{bmatrix} \begin{bmatrix} \boldsymbol{V}(d,s) \\ -\boldsymbol{I}(d,s) \end{bmatrix} \approx \begin{bmatrix} \boldsymbol{Q}_{11} & \boldsymbol{Q}_{12} \\ \boldsymbol{Q}_{21} & \boldsymbol{Q}_{22} \end{bmatrix} \begin{bmatrix} \boldsymbol{V}(0,s) \\ \boldsymbol{I}(0,s) \end{bmatrix} \quad (5)$$

where

$$\boldsymbol{Q}_{11} = \sum_{i=0}^{N} q_i \left[\frac{1}{2}(1+(-1)^i)(\boldsymbol{ab})^{i/2}\right]$$
$$\boldsymbol{Q}_{12} = \sum_{i=0}^{N} q_i \left[\frac{1}{2}(1-(-1)^i)(\boldsymbol{ab})^{(i-1)/2}\boldsymbol{a}\right]$$
$$\boldsymbol{Q}_{21} = \sum_{i=0}^{N} q_i \left[\frac{1}{2}(1-(-1)^i)(\boldsymbol{ba})^{(i-1)/2}\boldsymbol{b}\right]$$
$$\boldsymbol{Q}_{22} = \sum_{i=0}^{N} q_i \left[\frac{1}{2}(1+(-1)^i)(\boldsymbol{ba})^{i/2}\right] \quad (6)$$

and

$$\boldsymbol{a} = (\boldsymbol{R}+s\boldsymbol{L})d \quad \boldsymbol{b} = (\boldsymbol{G}+s\boldsymbol{C})d. \quad (7)$$

Subsequently, the form of the resulting Y parameters can be written as

$$\begin{bmatrix} \boldsymbol{I}_{(0,s)} \\ \boldsymbol{I}_{(d,s)} \end{bmatrix} = \begin{bmatrix} \boldsymbol{Y}_{11} & \boldsymbol{Y}_{12} \\ \boldsymbol{Y}_{21} & \boldsymbol{Y}_{22} \end{bmatrix} \begin{bmatrix} \boldsymbol{V}_{(0,s)} \\ \boldsymbol{V}_{(d,s)} \end{bmatrix}$$
$$\begin{bmatrix} \boldsymbol{Y}_{11} & \boldsymbol{Y}_{12} \\ \boldsymbol{Y}_{21} & \boldsymbol{Y}_{22} \end{bmatrix} = \Psi_1 + \Psi_2 = \begin{bmatrix} \boldsymbol{H}_w & -\boldsymbol{H}_w \\ -\boldsymbol{H}_w & \boldsymbol{H}_w \end{bmatrix} + \begin{bmatrix} \boldsymbol{H}_x & \boldsymbol{H}_x \\ \boldsymbol{H}_x & \boldsymbol{H}_x \end{bmatrix}$$
$$\boldsymbol{H}_w = \frac{1}{2}[\boldsymbol{Q}_{12}]^{-1}\boldsymbol{Q}_{11}$$
$$\boldsymbol{H}_x = \frac{1}{2}[\boldsymbol{Q}_{22}]^{-1}\boldsymbol{Q}_{21}. \quad (8)$$

The macromodels, such as the one described above and other passive macromodeling algorithms in the literature [7]–[10], efficiently capture the frequency response between (0 and $f_{\max}$). However, these macromodels may lead to significant high-frequency errors, causing faulty early-time responses. The reason for these errors is explained in Section III.

III. Concepts Pertinent to the Proposed Algorithm

A. Concept

For the early-time response to be reasonably flat (corresponding to the flat delay portion of the transmission-line response), it is desirable to have (as many as possible) initial derivatives of the impulse time response to be equal to zero. Note that the early-time impulse response is mainly influenced by the following relationship:

$$h(0^+) = \lim_{s\to\infty} sH_{MN}(s) \quad (9)$$

where s is the Laplace operator, $H_{MN}(s)$ represents the frequency-domain rational function, M is the numerator polynomial order, N is the denominator polynomial order, and $h(0^+)$

represents the early-time response (*around* $t = 0$). Next, assuming that $h(0^+) = 0$, the first derivative of the impulse response becomes

$$h^{(1)}(0^+) = \lim_{s\to\infty} s^2 H_{MN}(s). \tag{10}$$

Similarly, if the first p derivatives are zero, then the $h^{(p+1)}(0^+)$ can be expressed as

$$h^{(p+1)}(0^+) = \lim_{s\to\infty} s^{p+2} H_{MN}(s). \tag{11}$$

Observing (9)–(11), one can note that, to obtain flat response around $t = 0$ (i.e., to have as many as possible initial derivatives of the impulse time response to be equal to zero), the transfer-admittances represented by $H_{MN}(s)$ must satisfy $N > M$. This can be further illustrated using a numerical example as follows. For example, let the transfer-admittance Y_{12} of a transmission line be given by

$$y_{12} = \frac{1}{s^4 + 7s^3 + 17s^2 + 17s + 6} \tag{12}$$

then $y_{12}(0^+) = 0$, $y_{12}^{(1)}(0^+) = 0$, and $y_{12}^{(2)}(0^+) = 0$. Since the first few time derivatives of (12) are zero, the delay of the transmission line found in this case is reasonably approximated as a flat response. However, if the order of the numerator is much less than the order of denominator, then the rational approximation has fewer degrees of freedom to capture the frequency response. A practical compromise is to have the numerator be a few orders less than the denominator. This enables the transfer-admittance to have enough degrees of freedom, while ensuring that the first few derivatives are zero.

B. Limitations of Current Passive Macromodeling Algorithms

The current passive macromodeling algorithms, such as the one described by (5)–(8), efficiently capture the frequency response between (0 and $f_{\max}$). However, these macromodels can lead to significant high-frequency errors, causing faulty early-time response. The reason for these errors can be explained by noting the final rational forms of individual entries in the admittance matrix. For the sake of simplicity and without loss of generality, assume that the PUL parameters are scalars. For order N (*denoted as* $O(N)$), the orders of passive rational-form of Y parameters (8) are given by

$$\begin{bmatrix} \mathbf{Y}_{11} & \mathbf{Y}_{12} \\ \mathbf{Y}_{21} & \mathbf{Y}_{22} \end{bmatrix} \Rightarrow \begin{bmatrix} \frac{O(N)}{O(N-1)} & \frac{O(N)}{O(N-1)} \\ \frac{O(N)}{O(N-1)} & \frac{O(N)}{O(N-1)} \end{bmatrix} + \begin{bmatrix} \frac{O(N-1)}{O(N)} & \frac{O(N-1)}{O(N)} \\ \frac{O(N-1)}{O(N)} & \frac{O(N-1)}{O(N)} \end{bmatrix} \tag{13a}$$

$$\Rightarrow \frac{1}{O(2N-1)} \left\{ \begin{bmatrix} O(2N) & O(2N) \\ O(2N) & O(2N) \end{bmatrix} + \begin{bmatrix} O(2N-2) & O(2N-2) \\ O(2N-2) & O(2N-2) \end{bmatrix} \right\} \tag{13b}$$

$$\Rightarrow \begin{bmatrix} \frac{O(2N)}{O(2N-1)} & \frac{O(2N)}{O(2N-1)} \\ \frac{O(2N)}{O(2N-1)} & \frac{O(2N)}{O(2N-1)} \end{bmatrix}. \tag{13c}$$

As can be seen, the transfer admittances such as Y_{12} etc., have the rational form with orders $O(2N)/O(2N-1)$. Such a form arises mainly due to Theorem I, *which strictly requires the rational form of* $(N)/(N)$ *for the approximation of exponential matrix*. The above conclusion is true even for other types of passive macromodeling techniques in the literature [7]–[10], where the order difference between the denominator and numerator (i.e., N–M) ranges between -1 to 1. Obviously, transfer admittances of this form do not satisfy the conditions set by (9)–(11) (i.e., initial few derivatives of these transfer admittances are not equal to zero). Hence, these macromodels are susceptible to significant errors in the impulse transient response, especially in the early time region.

A further investigation of the rational form of Y parameters of (8) tells us why it is difficult to control the high-frequency response such that it satisfies the conditions required by (9)–(11) in order to produce a reasonably flat delay. For example, consider the case when N is even (without loss of generality) for a single conductor (with ground reference) transmission-line system. The corresponding rational function of the Y parameters (8) can be re-arranged as

$$\left.\begin{matrix} Y_{11} \\ Y_{22} \end{matrix}\right\} = \frac{Q_{11}Q_{22} + Q_{12}Q_{21}}{2Q_{12}Q_{22}} = \frac{\mu_N (ab)^N + \sum_{i=0}^{N-1} (\mu_i + \rho_i)(ab)^i}{a\left(\sum_{i=0}^{N-1} \varphi_i (ab)^i\right)}$$

$$\left.\begin{matrix} Y_{12} \\ Y_{21} \end{matrix}\right\} = \frac{-Q_{11}Q_{22} + Q_{12}Q_{21}}{2Q_{12}Q_{22}} = \frac{-\mu_N (ab)^N + \sum_{i=0}^{N-1} (-\mu_i + \rho_i)(ab)^i}{a\left(\sum_{i=0}^{N-1} \varphi_i (ab)^i\right)} \tag{14}$$

where the predetermined coefficients μ_i, ρ_i, and φ_i in (14) are obtained by the scalar approximation of (4) using the following relations:

$$\begin{aligned} \mathrm{Ev}(Q)\mathrm{Ev}(Q) &= \sum_{i=0}^{N} \mu_i s^{2i} \\ \mathrm{Odd}(Q)\mathrm{Odd}(Q) &= \sum_{i=0}^{N} \rho_i s^{2i} \\ 2\mathrm{Odd}(Q)\mathrm{Ev}(Q) &= \sum_{i=0}^{N-1} \varphi_i s^{(2i+1)}. \end{aligned} \tag{15}$$

Noticing (14), we can infer that, by appropriately choosing the values for ρ_i and μ_i such that $\mu_i = \rho_i$ (for example, $\mu_{N-1} = \rho_{N-1}$), the transfer admittances of (14) could be forced to have fewer polynomial terms on the numerator. However, since (14) does not have a ρ_N coefficient, it is very difficult to remove the highest order polynomial term. This implies that it is not possible to reduce the order of the numerator less than N without violating passivity conditions. In order to address these difficulties, we present a new algorithm in Section IV, which also provides a mechanism to control the asymptotic behavior of the high-frequency impulse response of the transfer admittance.

IV. Development of the Proposed Macromodeling Algorithm

The objective of the proposed algorithm is to provide a mechanism to control the macromodel impulse response beyond $f_{\max}$ so as to minimize early-time ripples while preserving the accuracy and passivity of the macromodel. For this purpose, the proposed algorithm uses two different orders of approximation of the scalar exponential in (4), $(N)/(N)$ and $(N+1)/(N+1)$ that satisfy Theorem 1. Consider a particular order N, if N is even (without loss of generality), then the approximation given by (4) can be expressed as

$$e^s \approx \frac{Q(s)}{Q(-s)} = \frac{\sum_{i=0}^{N} q_i s^i}{\sum_{i=0}^{N} q_i (-s)^i}. \tag{16}$$

Similarly, the other approximation corresponding to $N+1$ order can be denoted as

$$e^s \approx \frac{\tilde{Q}(s)}{\tilde{Q}(-s)} = \frac{\sum_{i=0}^{N+1} \tilde{q}_i s^i}{\sum_{i=0}^{N+1} \tilde{q}_i (-s)^i}. \tag{17}$$

Using the above two approximations, the rational approximation of (5) be expressed as

$$[\boldsymbol{Q}_{11} \quad -\boldsymbol{Q}_{12}] \begin{bmatrix} \boldsymbol{V}(d,s) \\ -\boldsymbol{I}(d,s) \end{bmatrix} \approx [\boldsymbol{Q}_{11} \quad \boldsymbol{Q}_{12}] \times \begin{bmatrix} \boldsymbol{V}(0,s) \\ \boldsymbol{I}(0,s) \end{bmatrix} \tag{18}$$

$$[-\tilde{\boldsymbol{Q}}_{21} \quad \tilde{\boldsymbol{Q}}_{22}] \begin{bmatrix} \boldsymbol{V}(d,s) \\ -\boldsymbol{I}(d,s) \end{bmatrix} \approx [\tilde{\boldsymbol{Q}}_{21} \quad \tilde{\boldsymbol{Q}}_{22}] \times \begin{bmatrix} \boldsymbol{V}(0,s) \\ \boldsymbol{I}(0,s) \end{bmatrix} \tag{19}$$

where the coefficients from (16) are used to approximate (18) and the coefficients from (17) are used to approximate (19). Note that the (18) and (19) are self consistent and do not violate the passivity conditions set by Theorem 1 [8]. The polynomial matrices $\boldsymbol{Q}_{11}$, $\boldsymbol{Q}_{12}$, $\tilde{\boldsymbol{Q}}_{21}$, and $\tilde{\boldsymbol{Q}}_{22}$ are now defined as

$$\begin{aligned}
\boldsymbol{Q}_{11} &= \sum_{i=0}^{N} q_i \left[\frac{1}{2}(1+(-1)^i)(\boldsymbol{ab})^{i/2}\right] \\
\boldsymbol{Q}_{12} &= \sum_{i=0}^{N} q_i \left[\frac{1}{2}(1-(-1)^i)(\boldsymbol{ab})^{(i-1)/2}\boldsymbol{a}\right] \\
\tilde{\boldsymbol{Q}}_{21} &= \sum_{i=0}^{N+1} \tilde{q}_i \left[\frac{1}{2}(1-(-1)^i)(\boldsymbol{ba})^{(i-1)/2}\boldsymbol{b}\right] \\
\tilde{\boldsymbol{Q}}_{22} &= \sum_{i=0}^{N+1} \tilde{q}_i \left[\frac{1}{2}(1+(-1)^i)(\boldsymbol{ba})^{i/2}\right].
\end{aligned} \tag{20}$$

Subsequently, the form of the resulting Y-parameters of (8) can be rewritten as

$$\begin{aligned}
\begin{bmatrix} \boldsymbol{Y}_{11} & \boldsymbol{Y}_{12} \\ \boldsymbol{Y}_{21} & \boldsymbol{Y}_{22} \end{bmatrix} &= \boldsymbol{\Psi_1} + \boldsymbol{\Psi_2} \\
&= \begin{bmatrix} \boldsymbol{H}_w & -\boldsymbol{H}_w \\ -\boldsymbol{H}_w & \boldsymbol{H}_w \end{bmatrix} + \begin{bmatrix} \tilde{\boldsymbol{H}}_x & \tilde{\boldsymbol{H}}_x \\ \tilde{\boldsymbol{H}}_x & \tilde{\boldsymbol{H}}_x \end{bmatrix} \\
\boldsymbol{H}_w &= \frac{1}{2}[\boldsymbol{Q}_{12}]^{-1}\boldsymbol{Q}_{11} \\
\tilde{\boldsymbol{H}}_x &= \frac{1}{2}[\tilde{\boldsymbol{Q}}_{22}]^{-1}\tilde{\boldsymbol{Q}}_{21}.
\end{aligned} \tag{21}$$

A. Single Transmission-Line Case

Consider the case of a single conductor (with ground reference) transmission-line system. Using (21), the rational function of Y-parameters can be expressed as

$$\begin{aligned}
\left.\begin{matrix} Y_{11} \\ Y_{22} \end{matrix}\right\} &= \frac{Q_{11}\tilde{Q}_{22} + Q_{12}\tilde{Q}_{21}}{2Q_{12}\tilde{Q}_{22}} = \frac{\sum_{i=0}^{N}(\mu_i + \rho_i)(ab)^i}{a\left(\sum_{i=0}^{N-1}\varphi_i(ab)^i\right)} \\
\left.\begin{matrix} Y_{12} \\ Y_{21} \end{matrix}\right\} &= \frac{-Q_{11}\tilde{Q}_{22} + Q_{12}\tilde{Q}_{21}}{2Q_{12}\tilde{Q}_{22}} = \frac{\sum_{i=0}^{N}(-\mu_i + \rho_i)(ab)^i}{a\left(\sum_{i=0}^{N-1}\varphi_i(ab)^i\right)}
\end{aligned} \tag{22}$$

where the predetermined coefficients μ_i, ρ_i, and φ_i in (22) are obtained using the relations

$$\begin{aligned}
\mathrm{Ev}(Q)\mathrm{Ev}(\tilde{Q}) &= \sum_{i=0}^{N} \mu_i s^{2i} \\
\mathrm{Odd}(Q)\mathrm{Odd}(\tilde{Q}) &= \sum_{i=0}^{N} \rho_i s^{2i} \\
2\mathrm{Odd}(Q)\mathrm{Ev}(\tilde{Q}) &= \sum_{i=0}^{N-1} \varphi_i s^{(2i+1)}.
\end{aligned} \tag{23}$$

B. Controlling the Asymptotic Behavior of the High-Frequency Impulse Response

Asymptotic behavior of the high-frequency impulse response can be controlled using the following mechanism. In formulation (22), the order of the numerator of the transfer-admittance can be reduced by appropriately choosing the values for ρ_i and μ_i. For example, while computing the predetermined constants, imposing the constraint

$$\mu_N = \rho_N \tag{24}$$

removes the highest order polynomial term of the transfer-admittance in (22) [i.e., *denominator order* − *numerator order* = 1 *in* (9)]. Similarly, imposing the constraints

$$\mu_N = \rho_N; \quad \mu_{N-1} = \rho_{N-1} \tag{25}$$

leads to the removal of two highest order polynomial terms of the numerator of the transfer admittance in (22) [i.e.,

$denominator\ order - numerator\ order = 3$ *in* (9)]. This makes the transfer admittance to satisfy the conditions set by (9)–(11). In other words, if a total number of k such constraints are used, then it ensures that the function and $2k-3$ derivatives of the transfer admittance are set to zero. For example, if $k=2$, then the order of transfer admittance y_{12} given by (22) is

$$\left.\begin{matrix} Y_{12} \\ Y_{21} \end{matrix}\right\} = \frac{\sum_{i=0}^{N-2} (-\mu_i + \rho_i) \left[(R+sL)(G+sC)d^2\right]^i}{(R+sL)d\left(\sum_{i=0}^{N-1} \varphi_i \left[(R+sL)(G+sC)d^2\right]^i\right)} \Rightarrow \frac{O(2N-4)}{O(2N-1)}. \tag{26}$$

In this case, using (9)–(11), we will have $y_{12}(0^+) = 0$ and $y_{12}^{(0)}(0^+) = 0$. It should be noted that if the number of constraints used in (25) is many and is comparable to the order of approximation, then the macromodel has fewer degrees of freedom to capture the frequency response. To obtain accurate macromodels, very few constraints should be used. For the examples provided in this paper, only one or two constraints were used, which provided significant improvement in the time-domain response.

C. Extension to Multiconductor Transmission Lines

Extension of the proposed algorithm to the case of multiconductor transmission lines can be explained as follows. Consider the Y-parameter terms of (21) for the case of single transmission line with ground reference. The submatrices H_w and $\tilde{H}_x$ can be expressed in terms of continued fraction expansion as

$$\begin{aligned} H_w =& \kappa_N b + \cfrac{1}{\kappa_{N-1}a + \cfrac{1}{\kappa_{N-2}b + \cdots \\ & \qquad \ddots \\ & \qquad \kappa_1 a}} \\ \tilde{H}_x =& \tau_{N+1} b + \cfrac{1}{\tau_N a + \cfrac{1}{\tau_{N-1}b + \cdots \\ & \qquad \ddots \\ & \qquad \tau_1 b}} \end{aligned} \tag{27}$$

where $a = R + sL$, $b = G + sC$. The coefficients κ and τ are the predetermined constants and are obtained using the continued-fraction representation of

$$\frac{\mathrm{Ev}(Q)}{2\mathrm{Odd}(Q)} = \kappa_N s + \cfrac{1}{\kappa_{N-1}s + \cfrac{1}{\kappa_{N-2}s + \cdots \\ \qquad \ddots \\ \qquad \kappa_1 s}} \tag{28}$$

$$\frac{\mathrm{Odd}(\tilde{Q})}{2\mathrm{Ev}(\tilde{Q})} = \tau_{N+1} s + \cfrac{1}{\tau_{N-1}s + \cfrac{1}{\tau_{N-2}s + \cdots \\ \qquad \ddots \\ \qquad \tau_1 s}} \tag{29}$$

where Q and $\tilde{Q}$ are described by (16) and (17). Next, from (21), the transfer admittances are given by

$$Y_{12} = Y_{21} = -H_w + \tilde{H}_x. \tag{30}$$

Hence, while computing the predetermined constants, if we impose the condition

$$\kappa_N = \tau_{N+1} \tag{31}$$

then it leads to the cancellation of the highest order polynomial term of the numerator of the transfer admittance of (22) [note that the condition set by (31) is also equivalent to setting $\mu_N = \rho_N$ as described by (24)]. Proceeding further, if we also make

$$\kappa_N = \tau_{N+1} \text{ and } \kappa_{N-1} = \tau_N \tag{32}$$

then it leads to the cancellation of the two highest polynomial terms, since the constraints of (32) are equivalent to the ones set by (24) ($\mu_N = \rho_N$ *and* $\mu_{N-1} = \rho_{N-1}$). If additional constraints of the type (32) are included during the computation of predetermined constants, then the order of the numerator of the transfer admittance can be reduced even further.

Using the similar approach discussed above, for the case of coupled lines, the submatrices of (21) can be expressed as

$$\begin{aligned} \boldsymbol{H}_w =& \kappa_N \boldsymbol{b} \\ & + \left(\kappa_{N-1}\boldsymbol{a} + \left(\cdots + \left(\kappa_2 \boldsymbol{b} + (\kappa_1 \boldsymbol{a})^{-1}\right)^{-1}\right)^{-1}\right)^{-1} \\ \tilde{\boldsymbol{H}}_x =& \tau_{N+1}\boldsymbol{b} \\ & + \left(\tau_N \boldsymbol{a} + \left(\cdots + \left(\tau_2 \boldsymbol{a} + (\tau_1 \boldsymbol{b})^{-1}\right)^{-1}\right)^{-1}\right)^{-1}. \end{aligned} \tag{33}$$

Next, imposing the constraints similar to (31) and (32) while computing the predetermined constants will help to control the asymptotic behavior of the transfer admittance. Note that the important advantage here, in the multiconductor admittance approximation given by (33), is that the predetermined coefficients κ_i and τ_i are obtained by the scalar approximation of (4).

D. Computation of Predetermined Coefficients

This section describes the formulation of the minimax objective function [8] for predetermining the coefficients of (16) and (17). The method imposes additional constraints to reduce the order of the numerator of transfer-admittance. The minimax objective function can be obtained by expressing the Nth and $(N+1)$th-order approximations given by (16) and (17) in terms of product of second-order factors as

$$e^s \approx \frac{Q(s)}{Q(-s)} = \frac{\prod_{i=1}^{N/2} (s^2 + g_{1,i}s + g_{0,i})}{\prod_{i=1}^{N/2} (s^2 - g_{1,i}s + g_{0,i})} \tag{34}$$

$$e^s \approx \frac{\tilde{Q}(s)}{\tilde{Q}(-s)} = \frac{(s+h_{0,0})\prod_{i=1}^{N/2} (s^2 + h_{1,i}s + h_{0,i})}{(-s+h_{0,0})\prod_{i=1}^{N/2} (s^2 - h_{1,i}s + h_{0,i})}. \tag{35}$$

Equations (34) and (35) satisfy the form of (4), which is required for passivity. Imposing the constraints that $g_{0,i}$, $g_{1,i}$, $h_{0,i}$, and $h_{1,i} > 0$ for all values of i ensures that the Hurwitz conditions of Theorem 1 are satisfied. Replacing $s = j\omega$, the minimax objective function can be written as

$$\max_{[0,\omega_{\max}]} \left(W_1(\omega) \left| e^{j\omega} - \frac{Q(j\omega)}{Q(-j\omega)} \right| + W_2(\omega) \left| e^{j\omega} - \frac{\tilde{Q}(j\omega)}{\tilde{Q}(-j\omega)} \right| \right) \text{ is minimum} \quad (36)$$

such that $g_{0,i}$, $g_{1,i}$, $h_{0,i}$, and $h_{1,i} > 0$ for all values of i. The variables $W_1(\omega)$, $W_2(\omega)$ are the weight functions at the angular frequency ω, where ω ranges from $0 \leq \omega \leq \omega_{\max} = 2\pi f_{\max}$. Imposing the following additional constraints ensures that the early-time ripples in transient responses are minimized

$$\begin{aligned} \kappa_N - \tau_{N+1} &= 0 \\ \kappa_{N-1} - \tau_N &= 0 \\ &\cdots \end{aligned} \quad (37)$$

where the κ's and the τ's are defined by (28) and (29) and can be expressed in terms of the g's and h's of (34) and (35). The number of constraints used in (37) will depend on the order of the approximation. For low orders, usually one constraint is needed. For higher order approximations, additional constraints may be required to control the asymptotic behavior of the high-frequency impulse response. It should be pointed out that if the number of constraints used in (37) is comparable to N (the order of approximation), then the macromodel becomes inefficient in capturing the frequency response, since it has less degrees of freedom. To obtain accurate macromodels, very few constraints should be used. For the examples provided in this paper, only one or two constraints were used, which provided significant improvement in the time-domain response.

It should be emphasized that the minimax optimization is performed on SCALAR functions of e^s and is independent of the number of coupled lines and the PUL parameters. The results obtained are then stored and the macromodel can be obtained analytically in terms of the predetermined coefficients and PUL parameters.

E. Preserving Passivity

Passivity is an important property to satisfy because macromodels that are stable, but not passive, can produce unstable networks when connected to other passive loads. This leads to spurious oscillations in simulation results. A linear n-port network with an admittance matrix $\boldsymbol{Y}(s)$ is said to be passive, if and only if [13]: 1) $\boldsymbol{Y}(s^*) = \boldsymbol{Y}^*(s)$ for all s, where $*$ is the complex conjugate operator and 2) $\boldsymbol{Y}(s)$ is a positive real matrix. That is the product $\boldsymbol{z}^{*t}[\boldsymbol{Y}^t(s^*) + \boldsymbol{Y}(s)]\boldsymbol{z} \geq 0$ for all possible values of s satisfying $\mathrm{Re}(s) > 0$ and for any arbitrary value of $\boldsymbol{z}$.

The first condition implies that the coefficients of the rational function matrix generated by the proposed macromodel must be real. The second condition implies that $\boldsymbol{Y}(s)$ must be a positive real matrix for all $\mathrm{Re}(s) > 0$. The coefficients generated by (21) are real values; therefore, the first condition of the passivity definition is always satisfied. The task that remains is to show that the Y-parameter matrix is positive real.

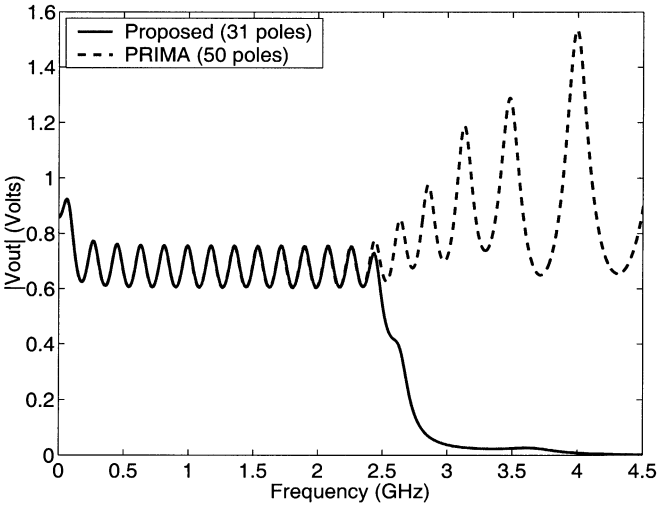

Fig. 1. Frequency response (Example 1).

In [8], it was shown that if the conditions of Theorem 1 are satisfied, then the matrices $\boldsymbol{\Psi_1}$ and $\boldsymbol{\Psi_2}$ of (8) are both positive real. The rational function $\boldsymbol{H}_w$ is formulated using the predetermined coefficients of (20). Since it is assumed that (16) satisfies the Hurwitz conditions of Theorem 1, it can be shown that $\boldsymbol{\Psi_1}$ is positive real, as demonstrated in [8]. Similarly, the rational function $\tilde{\boldsymbol{H}}_x$ is formulated by the predetermined coefficients of (17). Since it is assumed that (17) also satisfies the Hurwitz conditions of Theorem 1, it can be shown that $\boldsymbol{\Psi_2}$ is also positive real. The summation of two positive real matrices results in a positive real matrix which proves that the new macromodel is passive.

V. Computational Results

A. Example 1: Long Lossy Transmission Line

In this example, a long lossy distributed transmission-line network is analyzed with PRIMA [7] and the proposed algorithm. The near end is connected to a voltage source through a 5-Ω resistor and the far end is terminated with a 500-Ω resistor. The line is 40-cm long with PUL parameters of $R = 1.93\,\Omega$/cm, $L = 2.97$ nH/cm, $G = 79$ nS/cm, and $C = 1.61$ pF/cm. The frequency response at the far end of the transmission-line (V_{out}) is given in Fig. 1. Both approaches match the "original response" (obtained by directly solving Telegrapher's equations) up to 2.5 GHz, accurately, however, the high-frequency behavior beyond the matched frequency of 2.5 GHz is significantly different. Note that the proposed macromodel contains only 31 poles, whereas the PRIMA macromodel contains 50 poles (an equivalent 32-pole PRIMA macromodel matches the original response up to 1.6 GHz only). The transient response corresponding to PRIMA macromodel is given in Fig. 2. (The input is a pulse with a 0.35-ns rise/fall time and 1-ns pulsewidth; the label "IFFT" refers to inverse FFT of "original response" multiplied by the input frequency spectrum). The flat delay portion of the response from PRIMA suffers from spurious ripples. Fig. 3 gives the transient response of the proposed macromodel, and

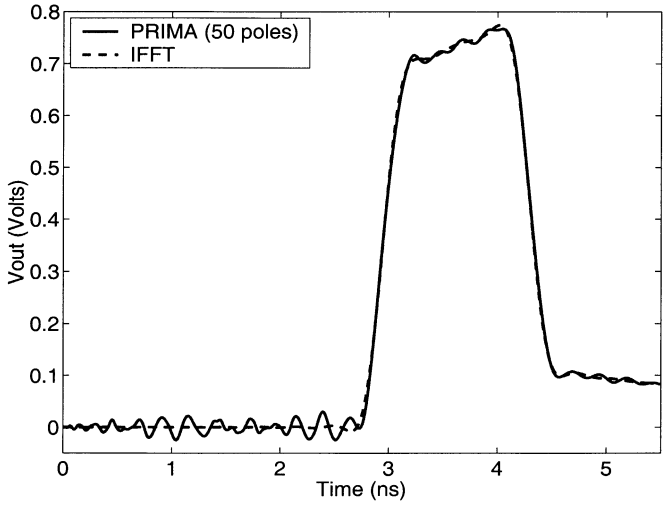

Fig. 2. Time response (IFFT versus PRIMA).

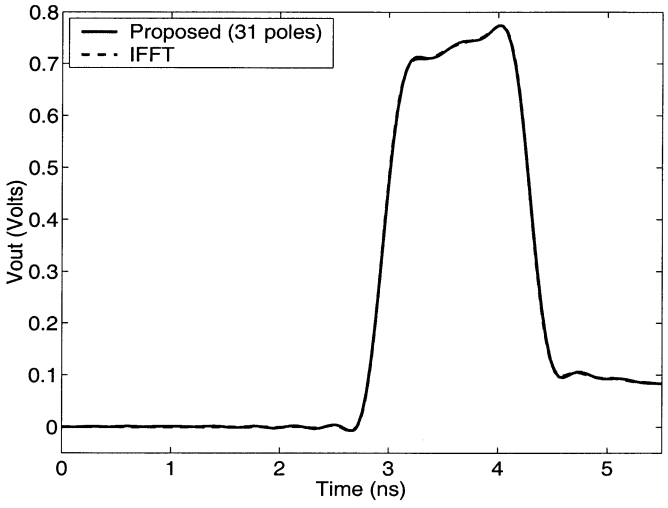

Fig. 3. Time response (IFFT versus proposed macromodel).

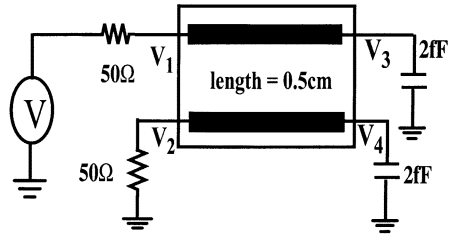

Fig. 4. Lossy coupled transmission-line network (Example 2).

it can be noticed that the spurious ripples in the flat-delay portion are significantly minimized. For this example, the predetermined coefficients of the proposed algorithm were obtained using two constraints ([i.e., $\kappa_N = \tau_{N+1}$, $\kappa_{N-1} = \tau_N$ in (37)].

B. Example 2: Lossy Coupled Transmission Line

A network with two lossy coupled transmission lines with frequency-dependent parameters is considered (Fig. 4). The length of the transmission-line network is 0.5 cm and the PUL parameters are described in Table I. The time-domain responses corresponding to an input step of 1 V and rise time of 0.07 ns at

TABLE I
PUL PARAMETERS OF EXAMPLE 2

Freq(GHz)	R_{11}(Ω/cm)	R_{22}(Ω/cm)	R_{12}(Ω/cm)	L_{11}(nH/cm)	L_{22}(nH/cm)	L_{12}(nH/cm)
0	54.980	333.700	0	14.024	14.1697	11.186
1.0e-3	56.440	335.550	1.4094	14.024	14.1697	11.186
3.3e-3	56.442	335.550	1.4130	14.023	14.1697	11.186
6.6e-3	56.447	335.556	1.4220	14.020	14.1607	11.178
1.0e-2	56.460	335.570	1.4320	14.000	14.1530	11.167
3.3e-2	56.677	335.785	1.4408	13.840	14.0030	11.012
6.6e-2	57.326	336.430	2.0620	13.365	13.5740	10.557
0.1	58.260	337.360	2.9540	12.710	12.9820	9.930
0.3	63.800	342.875	8.2570	9.3000	9.9040	6.676
0.66	68.337	347.375	12.560	7.1279	7.9456	4.603
1.0	70.375	349.380	14.454	6.5050	7.3840	4.009
3.5	77.443	356.416	20.320	5.6750	6.6450	3.226
6.6	84.188	363.250	24.549	5.5130	6.4960	3.087
10.0	92.682	371.725	29.190	5.4160	6.4090	3.018

$R_{12}=R_{21}$ $\qquad$ $L_{12}=L_{21}$

$$C = \begin{bmatrix} 1.79926 & 0.06759 \\ 0.06759 & 2.14866 \end{bmatrix} pF/cm \qquad G = \begin{bmatrix} 0 & 0 \\ 0 & 0 \end{bmatrix} S/cm$$

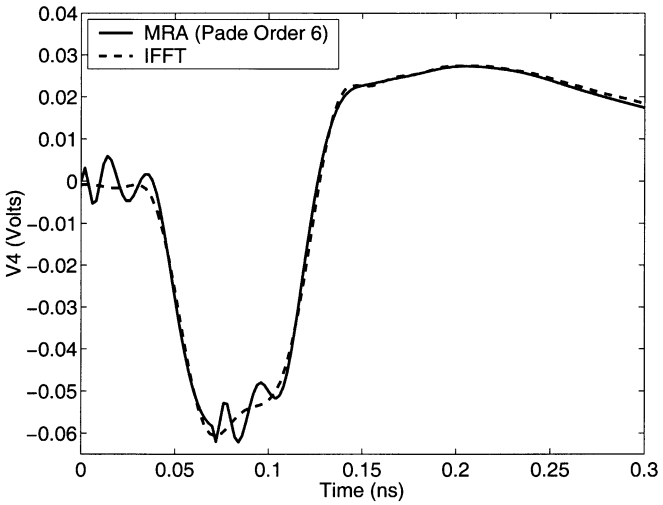

Fig. 5. Time response (IFFT versus MRA) (Example 2).

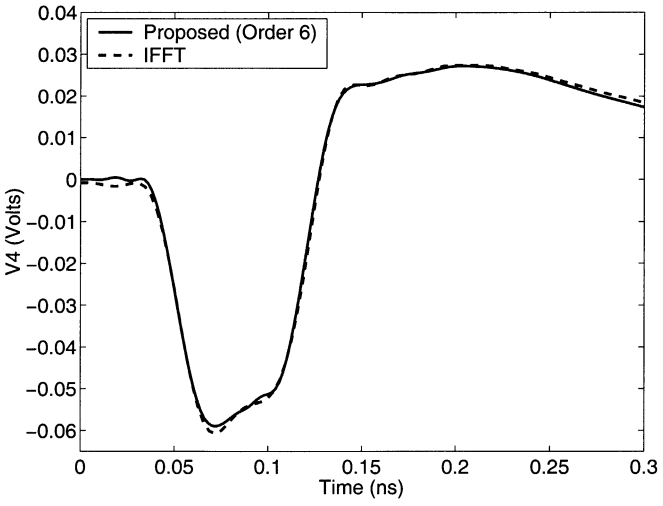

Fig. 6. Time response (IFFT versus proposed) (Example 2).

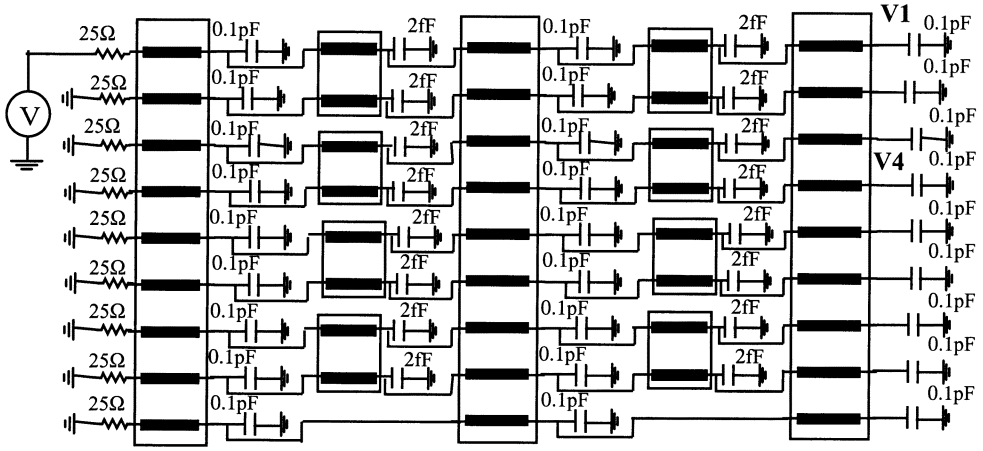

Fig. 7. Multiconductor transmission-line network (Example 3).

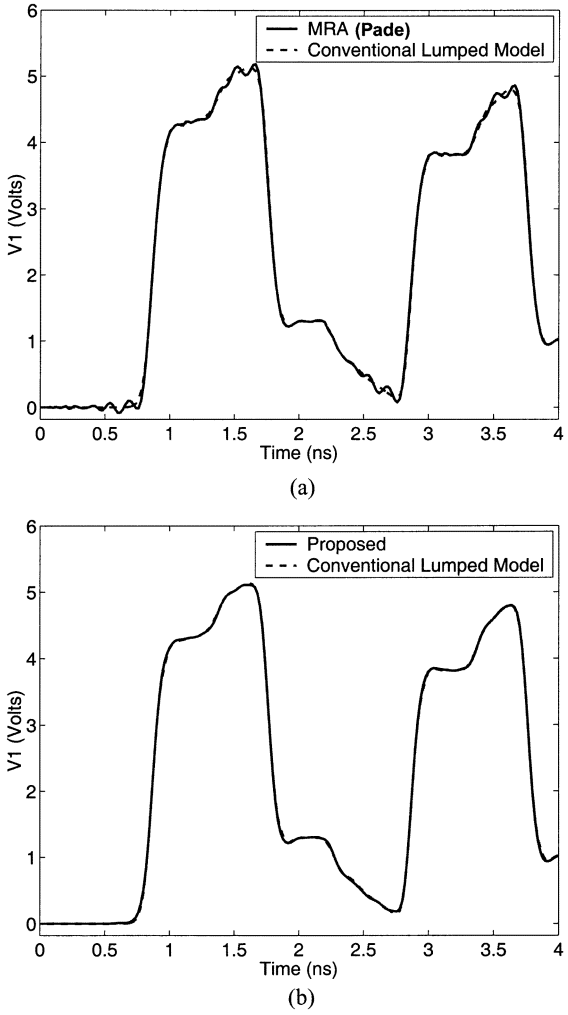

Fig. 8. Time-domain response at node V1 (Example 3).

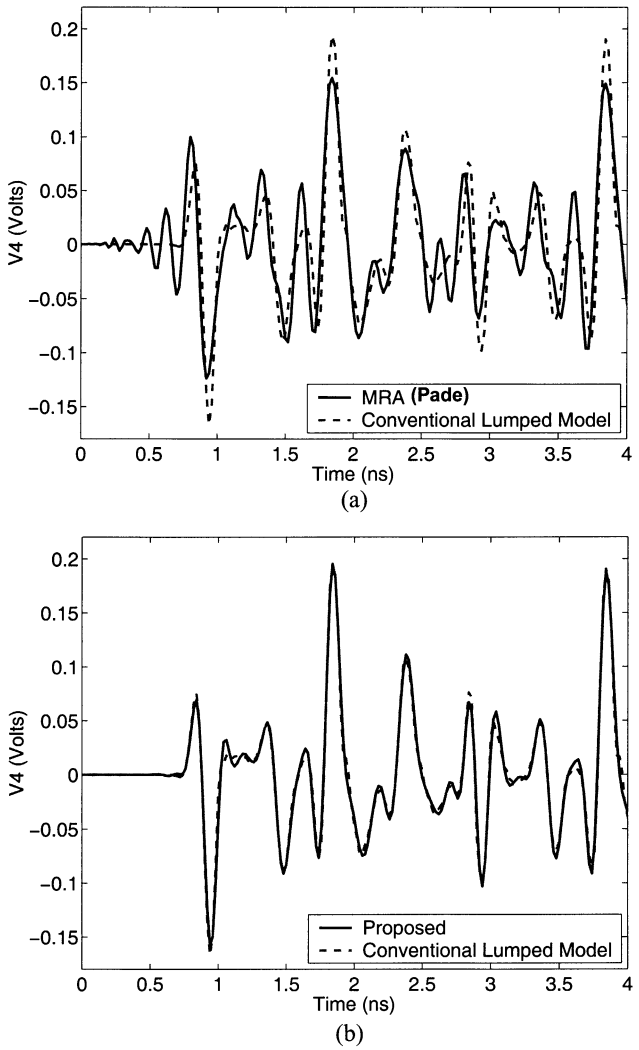

Fig. 9. Time-domain response at node V4 (victim line) (Example 3).

the victim node V4, using the MRA passive macromodel [8] and the proposed algorithm, are given in Figs. 5 and 6, respectively. As is seen, while matching the response accurately, the proposed algorithm minimized the early-time spurious ripples, considerably. For this example, the predetermined coefficients of the proposed algorithm were obtained using two constraints [i.e., $\kappa_N = \tau_{N+1}$, $\kappa_{N-1} = \tau_N$ in (37)].

C. Example 3: Multiconductor Transmission-Line Network

In this example, a relatively large interconnect system with several multiconductor transmission lines are considered (Fig. 7). Here, nine-coupled-transmission-line subnetworks have a length of 2.5 cm and the corresponding PUL parameters are as shown at the top of the following page.

$$L = \begin{bmatrix} 5.04 & 0.182 & 0.315 & 0.057 & 0.315 & 0.182 & 0.315 & 0.057 & 0.315 \\ 0.182 & 5.04 & 0.315 & 0.182 & 0 & 0 & 0 & 0 & 0.315 \\ 0.315 & 0.315 & 5.04 & 0.315 & 0.182 & 0 & 0.057 & 0 & 0.182 \\ 0.057 & 0.182 & 0.315 & 5.04 & 0 & 0 & 0 & 0 & 0 \\ 0.315 & 0 & 0.182 & 0 & 5.04 & 0.315 & 0.182 & 0 & 0 \\ 0.182 & 0 & 0 & 0 & 0.315 & 5.04 & 0.315 & 0.182 & 0 \\ 0.315 & 0 & 0.057 & 0 & 0.182 & 0.315 & 5.04 & 0.315 & 0.182 \\ 0.057 & 0 & 0 & 0 & 0 & 0.182 & 0.315 & 5.04 & 0 \\ 0.315 & 0.315 & 0.182 & 0 & 0 & 0 & 0.182 & 0 & 5.04 \end{bmatrix} \text{ nH/cm}$$

$$C = \begin{bmatrix} 187.6 & -0.385 & -2.23 & -0.0046 & -2.23 & -0.385 & -2.23 & -0.0046 & -2.23 \\ -0.385 & 187.6 & -2.23 & -0.385 & 0 & 0 & 0 & 0 & -2.23 \\ -2.23 & -2.23 & 187.6 & -2.23 & -0.385 & 0 & -0.0046 & 0 & -0.385 \\ -0.0046 & -0.385 & -2.23 & 187.6 & 0 & 0 & 0 & 0 & 0 \\ -2.23 & 0 & -0.385 & 0 & 187.6 & -2.23 & -0.385 & 0 & 0 \\ -0.385 & 0 & 0 & 0 & -2.23 & 187.6 & -2.23 & -0.385 & 0 \\ -2.23 & 0 & -0.0046 & 0 & -0.385 & -2.23 & 187.6 & -2.23 & -0.385 \\ -0.0046 & 0 & 0 & 0 & 0 & -0.385 & -2.23 & 187.6 & 0 \\ -2.23 & -2.23 & -0.385 & 0 & 0 & 0 & -0.385 & 0 & 187.6 \end{bmatrix} \text{ pF/m}$$

TABLE II
CPU COMPARISON FOR EXAMPLE 3

Algorithm	Total number of lumped sections	CPU time (SPARC Ultra 5-10) (seconds)
Conventional Lumped	1606	470
Proposed	221	76

The two-coupled-transmission-line subnetworks have a length of 0.4 cm and their PUL parameters are the same as that described in example 2 (Table I). The transient responses corresponding to an input pulsewidth of 0.8 ns, a rise/fall time of 0.1 ns, and a period of 2 ns are shown in Figs. 8 and 9. Table II compares the total number of segments of the entire network and the CPU time for the proposed and conventional lumped model. For their respective orders, both the proposed and conventional lumped model give similar time-domain responses. However, the proposed method is about six times faster. In addition, the proposed method is able to achieve better accuracy than the MRA macromodel [8] for equal-order approximations (see the comparison in Figs. 8 and 9). The accuracy improvement of the proposed method is especially noticeable for weak signals such as the transient responses of the victim line at node V4 (Fig. 9). For this example, the predetermined coefficients of the proposed algorithm were obtained using one constraints [i.e., $\kappa_N = \tau_{N+1}$, $\kappa_{N-1} = \tau_N$ in (37)].

VI. CONCLUSIONS

In this paper, a new algorithm is presented for accurate passive macromodeling of distributed transmission-line networks. The algorithm provides a mechanism to control the asymptotic behavior of the high-frequency impulse response, while matching the response up to $f_{\max}$ accurately. This results in significant reduction in early-time spurious ripples in transient responses. It is to be noted that the principles stated in this paper are general in nature and can be included in other rational-function-based passive macromodeling algorithms available in the literature, with appropriate modifications.

ACKNOWLEDGMENT

The authors acknowledge I. M. Elfadel and A. E. Ruehli of IBM T. J. Watson Research Center, Yorktown Heights, NY, and H.-M. Huang of IBM Microelectronics Division, Hopewell Junction, NY, for several useful technical discussions and for providing the test examples.

REFERENCES

[1] C. R. Paul, *Analysis of Multiconductor Transmission Lines*. New York: Wiley, 1994.
[2] R. Achar and M. Nakhla, "Simulation of high speed interconnects," *Proc. IEEE*, vol. 89, pp. 693–728, May 2001.
[3] F. H. Branin Jr., "Transient analysis of lossless transmission lines," *Proc. IEEE*, vol. 55, pp. 2012–2013, Nov. 1967.
[4] A. J. Gruodis and C. S. Chang, "Coupled lossy transmission line characterization and simulation," *IBM J. Res. Develop.*, vol. 25, pp. 25–41, Jan. 1981.
[5] F. Y. Chang, "The generalized method of characteristics for wave-form relaxation analysis of coupled transmission lines," *IEEE Trans. Microwave Theory Tech.*, vol. 37, pp. 2028–2038, Dec. 1989.
[6] S. Lin and E. S. Kuh, *The Complete Multimedia Book Series on Signal Integrity (High-Speed Circuit and Interconnect Analysis)*. Ottawa, ON, Canada: OMNIZ Global Knowledge Corporation, 2002. [Online] Available: http://www.omniz.com.
[7] A. Odabasioglu, M. Celik, and L. T. Pilleggi, "PRIMA: Passive reduced-order interconnect macromodeling algorithm," *IEEE Trans. Computer-Aided Design*, vol. 17, pp. 645–654, Aug. 1998.
[8] A. Dounavis, R. Achar, and M. Nakhla, "Passive macromodels for distributed high-speed networks," *IEEE Trans. Microwave Theory Tech.*, vol. 11, pp. 1686–1696, Oct. 2001.
[9] Q. Yu, J. M. L. Wang, and E. S. Kuh, "Passive multipoint moment matching model order reduction algorithm on multiport distributed interconnect networks," *IEEE Trans. Circuits Syst. I*, vol. 46, pp. 140–160, Jan. 1999.
[10] A. Cangellaris, S. Pasha, J. Prince, and M. Celik, "A new discrete time-domain model for passive model order reduction and macromodeling of high-speed interconnections," *IEEE Trans. Comp. Packag. Technol.*, vol. 22, pp. 356–364, Aug. 1999.

[11] I. Elfadel, H. Huang, A. Ruehli, A. Dounavis, and M. Nakhla, "A comparative study of two transient analysis algorithms for lossy transmission lines with frequency-dependent data," in *Proc. 10th Topical Meeting on EPEP*, Oct. 2001, pp. 255–258.

[12] A. Dounavis, R. Achar, and M. Nakhla, "On passive time-domain macromodels of distributed transmission-line networks," in *Dig. IEEE Int. Microwave Symp.*, vol. 2, June 2002, pp. 975–978.

[13] E. S. Kuh and R. A. Rohrer, *Theory of Linear Active Networks*. San Francisco, CA: Holden-Day, 1967.

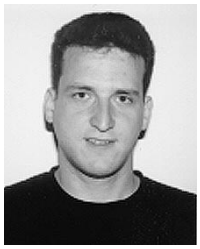

Anestis Dounavis (S'99) received the B.Eng. degree from McGill University, Montreal, QC, Canada, in 1995 and the M.Eng degree in 2000 from Carleton University, Ottawa, ON, Canada, where he is currently working toward the Ph.D. degree in the Department of Electronics.

His research interests include CAD design of VLSI systems, high-frequency interconnects, and numerical algorithms.

Mr. Dounavis received the Carleton University Medal for his Master's thesis on time-domain macromodeling of high-speed interconnects.

Ramachandra Achar (S'95–M'00) received the B.Eng. degree in electronics engineering from Bangalore University, Bangalore, India in 1990, the M.Eng. degree in micro-electronics from Birla Institute of Technology and Science, Pilani, India, in 1992, and the Ph.D. degree from Carleton University, Ottawa, ON, Canada, in 1998.

He is currently an Assistant Professor in the Department of Electronics, Carleton University. During 1998–2000, he served as a Research Engineer in the CAE Group at Carleton University. He was previously with Larsen and Toubro Engineers Ltd., Mysore, India, and the Indian Institute of Science, Bangalore, India, as an Research and Development Engineer. He spent the summer of 1995 working on the macromodel development for high-speed linear circuits at T. J. Watson Research Center, IBM, NY. His research interests include modeling and simulation of high-speed interconnects, numerical algorithms, and development of CAD tools for high-frequency circuit analysis.

Dr. Achar is the recipient of several prestigious awards, including the Natural Science and Engineering Research Council (NSERC) doctoral award (2000), the Strategic Microelectronics Corporation (SMC) Award (1997), Canadian Microelectronics Corporation (CMC) Award (1996), and the Best Student Paper Award from the 1998 Micronet (a Canadian Network of Centres of Excellence on Microelectronics) annual workshop. He also received the University Medal for his doctoral work on high-speed VLSI interconnect analysis from Carleton University.

Michel S. Nakhla (F'98) received the M.A.Sc. and Ph.D. degrees in electrical engineering from University of Waterloo, ON, Canada, in 1973 and 1975, respectively.

During 1976-1988, he was with Bell-Northern Research, Ottawa, ON, Canada, as Senior Manager of the computer-aided engineering group. In 1988, he joined Carleton University, Ottawa, ON, Canada as a Professor and the holder of the Computer-Aided Engineering Senior Industrial Chair, established by Nortel Networks and the Natural Sciences and Engineering Research Council of Canada. He is currently a Professor of Electrical Engineering. He is the founder of the high-speed CAD research group at Carleton University and is a frequent invited speaker on the topic of high-speed interconnects. He serves as a Technical Consultant for several industrial organizations and is the principal investigator for several major sponsored research projects. His research interests include CAD of VLSI and microwave circuits, modeling and simulation of high-speed interconnects, nonlinear circuits, multidisciplinary optimization, thermal and electromagnetic emission analysis, and MEMS and neural networks.